Cement and Concrete Research 40 (2010) 253–259

Contents lists available at ScienceDirect

Cement and Concrete Research

journal homepage: http://ees.elsevier.com/CEMCON/default.asp

Interaction between α-calcium sulfate hemihydrate and superplasticizer from the point of adsorption characteristics, hydration and hardening process

Baohong Guan, Qingqing Ye, Jiali Zhang, Wenbin Lou, Zhongbiao Wu *

Department of Environmental Engineering, Zhejiang University, Hangzhou 310027, China

ARTICLE INFO

Article history:
Received 9 December 2008
Accepted 21 August 2009

Keywords:
α-calcium sulfate hemihydrate (D)
Superplasticizer (D)
Adsorption (C)
Hydration (A)
Hardening (A)

ABSTRACT

Superplasticizers (SPs), namely sulfonated melamine formaldehyde (SMF) and polycarboxylate (PC), were independently admixed with α-calcium sulfate hemihydrate based plaster to improve the material's performance. SMF and PC gave, respectively, 38% and 25% increases in the 2 h bending strength at the optimum dosages of 0.5 wt.% and 0.3 wt.%, which are determined essentially by the maximum water-reducing efficiency. The peak shift of binding energy of $Ca2p_{3/2}$ detected by X-ray photoelectron spectroscopy (XPS) suggests that SPs are chemically adsorbed on gypsum surface. A careful examination of the strength development of set plaster allowed the hydration and hardening process to be divided roughly into five stages. SMF accelerates early hydration, while PC decelerates it. Both SPs allowed similar maximum water reductions, giving a more compact structure and a decrease in total pore volume and average pore diameter, and thus leading to higher strengths in the hardened plasters with SPs.

1. Introduction

Superplasticizers (SPs) are widely used as additives to reduce water demand and improve workability of cementitious materials, leading to higher strength and better durability of the hardened products. Sulfonated melamine formaldehyde (SMF) represents a traditional class of SP, while polycarboxylate (PC) is a relatively new class of SP. Both types have been widely applied in cement and concrete [1,2]. Different effects are often exhibited when the same material is modified with different SPs. These can be attributed to differences in "compatibility" between SP and material being modified.

Gypsum plasters are another important class of cementitious material, different from cement and concrete. However, application of SP to gypsum plasters largely lags behind. Some work has been done on β-calcium sulfate hemihydrate (β-HH) which is commonly known as plaster of Paris [3–5]. Another form of hemihydrate, α-calcium sulfate hemihydrate (α-HH), has much higher value than β-HH owing to its better performance, such as lower water demand, faster setting [6] and higher strength [7]. α-HH has been widely applied in precision instrument moulds, ceramics, industrial arts and architecture. SPs used in cement, concrete and plaster of Paris may not be compatible with α-HH based plaster. In fact, the interactions between α-HH and SP are not well known.

In this study, the compatibility of α-HH with SMF or PC is examined by focusing on the adsorption characteristics, hydration and hardening processes of the SP-modified plasters.

2. Materials and methods

The raw material is a commercial product prepared by solid autoclaving method, with an α-HH content of 95 wt.%. Particle size distribution of the plaster is shown in Fig. 1. The characteristic particle sizes of the material are: $d_{10} = 2.2$ μm, $d_{50} = 29.3$ μm, and $d_{90} = 97.7$ μm, respectively. SMF and PC are both commercial products. SMF has an average molecular weight of 10,000 and an acidity index of 14.55 mg NaOH/g, while PC has an average molecular weight of 1200 and an acidity index of 18.65 mg NaOH/g. The characteristics of the SPs are shown in detail in Table 1.

The sample was modified by mixing SP with α-HH powder manually in a beaker for 30 s, then the powder was blended with water in a mixer at 400 rpm for 30 s until a homogenous paste was produced. The preparation of paste was carried out at the water–hemihydrate weight ratio (W/H) giving standard consistency, unless specifically noted.

The W/H for standard consistency and setting time of plaster was tested according to GB/T 17669.4 (China national standard for gypsum plasters). The W/H for standard consistency of this plaster was 0.32. The paste was cast into three 20 mm × 20 mm × 80 mm iron moulds and compacted by jolting. Maintained for 30 min, the prisms were demoulded and stored in a curing chest maintained at (20 ± 2)°C and (65 ± 5) %RH. At certain ages, the prisms were tested for bending strength under three-point loading with a span of 50 mm and a loading rate of 0.02 kN/s. The broken half pieces were tested for compressive strength with area loading of 0.0004 m^2 and loading rate of 0.6 kN/s.

5 min after α-HH mixing with water, the paste was dipped in anhydrous ethanol to terminate hydration. Then, the sample was

* Corresponding author. Tel.: +86 571 88273650; fax: +86 571 88273687.
E-mail address: zbwu@zju.edu.cn (Z. Wu).

0008-8846/$ – see front matter © 2009 Elsevier Ltd. All rights reserved.
doi:10.1016/j.cemconres.2009.08.027

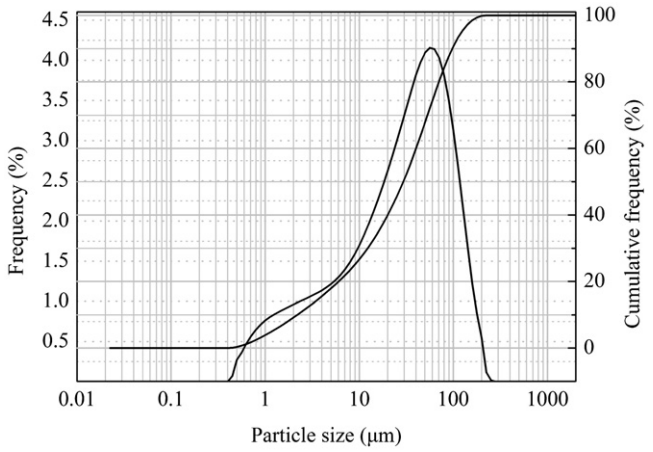

Fig. 1. Particle size distribution of α-calcium sulfate hemihydrate (α-HH) based plaster.

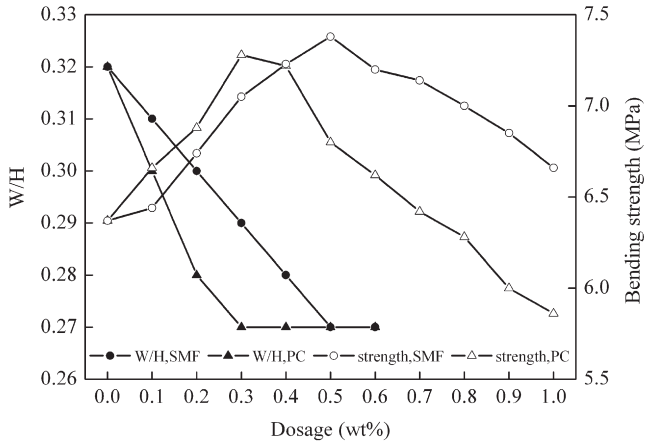

Fig. 2. Effect of superplasticizers (SPs) on the water–hemihydrate weight ratio (W/H) for standard consistency and the 2 h bending strength of α-calcium sulfate hemihydrate (α-HH) based plasters at W/H of 0.32.

dried in a vacuum oven (10^{-1} bar) at 45 °C until mass stabilization and cooled in a desiccator. X-ray photoelectron spectroscopy (XPS) measurement was performed with Thermo ESCALAB 250 spectrometer aided by Ar-ion etching analyzer. A monochromatic Al-Kα radiation source ($h\nu = 1486.6$ eV) was used at a spot size of 500 μm. The analyzer worked in a constant resolution mode at pass energy of 20 eV. The full width at half maximum (FWHM) of $Ag3d_{5/2}$ peak of 0.6 eV was determined from a clean silver specimen. The XPS lines were calibrated using C1s line at 284.8 eV. Survey and high-resolution spectra of Ca2p, S2p, and N1s were recorded. The atomic concentration was calculated from the total peak area of the characteristic peak using the elemental sensitivity factor.

At various times the hydration of paste was terminated and the crystal water content of the hydration products was determined by thermogravimetry (NETZSCH STA 409PC Luxx) under N_2 gas atmosphere with a heating rate of 10 °C/min and a gas flow of 20 ml/min.

To monitor the temperature variation during hydration, 200 g powder was evenly blended with water at W/H = 0.27 and 0.32 for 30 s. The resulting paste was immediately poured into the disposable lining of a homemade semi-adiabatic calorimeter, after which a temperature probe (with sleeve) was immersed into the paste. In the experiment, the temperature of the thermos vessel was adjusted to the ambient temperature (20 °C), so did the materials. Time constant, τ, is the parameter of the exponential cooling curve. Calculation of τ was carried out for each sample tested by spontaneous cooling at the end of the hydration period. The time constants of this semi-adiabatic calorimeter are determined to be nearly 1.7 h in the case of set plasters with or without modification at W/H = 0.32.

2 h after mixing with water, the hydration of an α-HH paste was terminated, and the crystal morphology of the product was analyzed by Scanning Electron Microscope (SEM, HITACHI S-570). BET surface area, total pore volume and average pore diameter of set plaster after 7 days of hydration and hardening were determined by MICROMERITICS ASAP 2010 M+C with nitrogen full adsorption at 77 K bath temperature using BET and BJH methods.

3. Results and discussion

3.1. Dosage optimization of SPs

The effect of SPs on the W/H for standard consistency and the 2 h bending strength of set plaster are presented in Fig. 2. SPs significantly lower the W/H for standard consistency from 0.32 to 0.27, as SPs increase from 0 to 0.5 wt.% for SMF and to 0.3 wt.% for PC, respectively. More SPs do not further lower the W/H. It indicates that the maximum water-reducing efficiency of SMF or PC for α-HH based plaster is 15.6%. Thus, the optimum dosage is 0.5 wt.% for SMF and 0.3 wt.% for PC, respectively.

The 2 h bending strength of set plaster initially increases with SP dosage, due to the reduction in W/H. An inflexion denoting the maximum water reduction (to W/H = 0.27) at 0.5 wt.% SMF or 0.3 wt.% PC, and then the strength declines sharply with increasing SP dosage, because the W/H could not be reduced any further if a castable fresh plaster was required. At any given W/H, the higher the SP dosage, the greater the amount adsorbed on the growing gypsum crystals, leading to reduced crystal–crystal bonding and thus lower strengths [8]; but our results show that, up to the maximum effective water reduction level, the strength increase due to reduced W/H was greater than the strength decrease due to reduced inter-crystallite bonding. Therefore, under practically-useful conditions the optimum dosage of SMF or PC for α-HH based plaster is determined essentially by the maximum water-reducing efficiency of the SPs.

3.2. Adsorption characteristics of SPs

The functional ion groups of SP molecules are believed to form complexes with Ca^{2+} in the aqueous phase of gypsum plasters. When SMF reacts with Ca^{2+}, R-SO_3Na transforms to $(R\text{-}SO_3)_2Ca$ [9]. When

Table 1
Superplasticizers (SPs) characteristics.

Superplasticizer	Appearance	Average molecular weight	pH value (20 °C)	Water content (%)	Content of $[SO_4]^{2-}$ (%)	Content of Cl^- (%)	Bulk density (kg m^{-3})	Acidity index (mg NaOH/g SP)
SMF	White powder	10,000	7–9 (c = 5%, in aqueous solution)	5 ± 1	3–4	≤0.5	500–600	14.55
PC	Light gray powder	1200	6–8 (c = 20%, in aqueous solution)	<3	2.6	0.01	500–600	18.65

PC is added to cement pastes containing $[SO_4]^{2-}$, a competitive adsorption of Ca^{2+} by PC and $[SO_4]^{2-}$ is observed [10]. The binding energy of $Ca2p_{3/2}$ peak for $CaSO_4$ is nearly 347.5 eV [11]. Fig. 3 shows $Ca2p_{3/2}$ scan XPS spectra on both an argon ion-etched surface where no functional ion groups of SP can be found, and un-etched gypsum surfaces from both SP-modified set plasters, representing respectively the spectra before and after adsorption. The peak of binding energy of $Ca2p_{3/2}$ is observed to be shifted by about 0.65 eV to the higher energy region by adsorption of SPs, indicating that SMF and PC are both chemically adsorbed on gypsum surface in the form of monolayer, with a small amount adsorbed. The shift to higher energy region implies a stronger binding between electrons in inner orbit and nucleus, which results from the loss or partial decrease of valence electrons. It seems that the higher electronegativity of the functional ion groups of SPs (mainly, $[R\text{-}SO_3]^-$ in SMF, $[R\text{-}COO]^-$ and $[R\text{-}SO_3]^-$ in PC) must be responsible for this phenomenon.

The intensity of the $Ca2p_{3/2}$ peak was increased by SMF, and decreased by PC. The addition of excess PC has a stronger negative impact on the strength of set plaster than the addition of excess SMF. It is very likely that the SPs have various adsorption conformations. SMF is lying on material surface and its dispersion capacity presumably depends mainly on the electrostatic repulsive force produced by the adsorption double electrical layer [12]. The PC is a comb-shaped polymer, and its dispersion ability comes from a combination effect of steric hindrance and electrostatic repulsive force [5,13]. The electrostatic repulsive force which is easily affected by the rapid hydration of plaster is less stable than the steric hindrance. Owing to strong steric hindrance generated by the side chains of PC, the water-reducing capacity of PC is higher than that of SMF.

The atomic composition on gypsum surface varies with the dosage of SP, as shown in Table 2. Reaction of $[R\text{-}SO_3]^-$ in SPs with Ca^{2+} plays an important role in the variation of Ca2p/S2p ratio. The ratio for $Ca^{2+}/2[R\text{-}SO_3]^-$ is 0.50, while it is 1.00 for pure set plaster. We observe that the Ca2p/S2p ratio decreases with increasing SMF dosage until it apparently reaches saturation at about 0.5 wt.% SMF. In the case of PC-modified plaster, the variation of the Ca2p/S2p ratio is in the range of 0.96–1.02, as a result of Ca^{2+} bonding with both of $[R\text{-}COO]^-$ and $[R\text{-}SO_3]^-$, which provides less information about the optimum dosage.

No nitrogen can be detected on the surfaces of pure plaster and PC-modified plaster. But the SMF-modified plaster is characterized by N atoms from the SMF. The variation of the Ca2p/N1s ratio is also used to indicate the adsorption property of SMF. The Ca2p/N1s ratio decreases sharply from 6.03 to 2.54 as SMF increases from 0.3 wt.% to 0.5 wt.%, and then decreases gently to 1.77 at 0.7 wt.% SMF. Since there is more N than S in SMF, the Ca2p/N1s ratio varies more strongly with increasing SMF than the Ca2p/S2p ratio. The above results support the idea that the optimum dosage of SMF for α-HH based plaster is determined by the saturated adsorption amount of SMF on the gypsum surface.

Table 2
Variation of atomic composition on gypsum surface of modified set plasters with different dosage of superplasticizers (SPs) at water–hemihydrate weight ratio (W/H) of 0.32.

Item		Ar—20 nm (no SP)	SMF (wt.%)			PC (wt.%)		
			0.3	0.5	0.7	0.1	0.3	0.5
Ratio of atomic concentration	Ca2p/S2p	1.00	0.97	0.91	0.90	0.97	1.02	0.96
	Ca2p/N1s	–	6.03	2.54	1.77	–	–	–

Note: No nitrogen can be detected in pure plaster and PC-modified plaster, remarked as "–".

3.3. Hydration process of plaster

The hydration of α-HH can be described as:

$$CaSO_4 \cdot 0.5H_2O + 1.5H_2O = CaSO_4 \cdot 2H_2O + Q.$$

Thus, the evolution of the crystal water content of the hydration product or heat generation during hydration can be used to follow the process.

As shown in Fig. 4, the hydration is quite fast during the first 20 min, and then it slows down. For the pure plaster at W/H = 0.32, it takes 8 h to complete the transformation from α-HH to calcium sulfate dihydrate (DH) and it is about 72% complete after 2 h at 20 °C. Comparatively, for the 0.5 wt.% SMF-modified plaster at W/H = 0.27, it takes only 6 h to complete the hydration and it is 80% complete at 2 h. The hydration of 0.3 wt.% PC-modified plaster appears slower, it takes 8 h to complete hydration and the hydration degree at 2 h is even lower than that of the pure plaster.

Semi-adiabatic calorimetry was helpful in allowing us to compare the kinetics of hydration of the paste over a range of W/H ratios and SP dosages. Since the majority of the hydration occurs within the first 2 h, the temperature changes intensely during this period, as shown in Fig. 5. The hydration is an exothermic process and it can reasonably be assumed that the molar enthalpy change for the reaction is identical for the pure plaster and the SP-modified plasters. In this semi-adiabatic calorimeter the temperature peak of the pure plaster at W/H = 0.32 appears at about 1.5 h. It shifts ahead slightly (by about

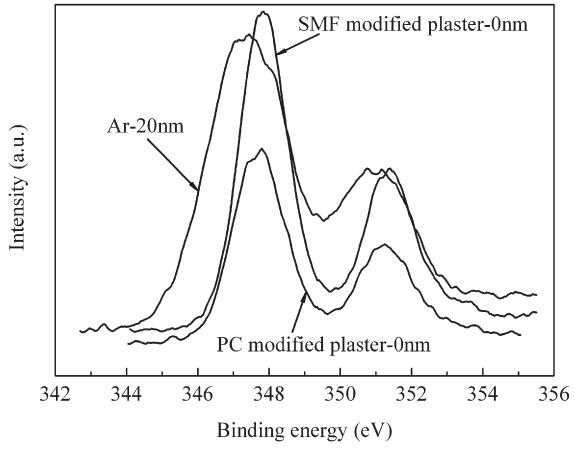

Fig. 3. $Ca2p_{3/2}$ scan XPS spectra on etched surface (depth: 20 nm) and gypsum surface of modified set plasters at water–hemihydrate weight ratio (W/H) of 0.32, dosage: sulfonated melamine formaldehyde (SMF) 0.5 wt.%, polycarboxylate (PC) 0.3 wt.%.

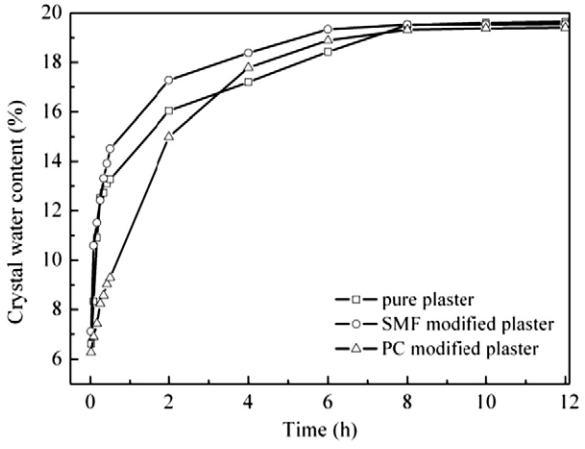

Fig. 4. Crystal water content evolution of hydration product during α-calcium sulfate hemihydrate (α-HH) hydration, water–hemihydrate weight ratio (W/H): pure plaster 0.32, modified plasters 0.27; dosage: sulfonated melamine formaldehyde (SMF) 0.5 wt.%, polycarboxylate (PC) 0.3 wt.%.

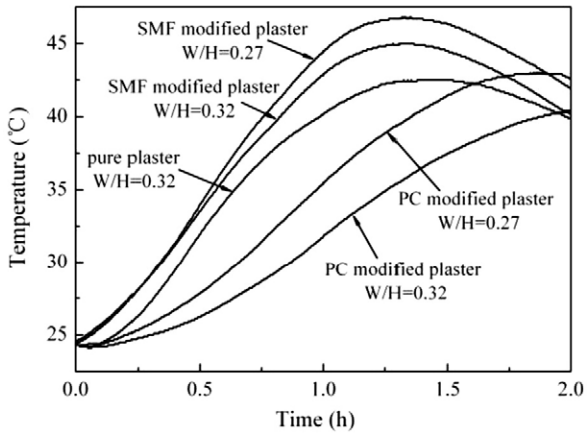

Fig. 5. Heat evolution during α-calcium sulfate hemihydrate (α-HH) hydration, water–hemihydrate weight ratio (W/H): pure plaster 0.32, modified plasters 0.27, 0.32; dosage: sulfonated melamine formaldehyde (SMF) 0.5 wt.%, polycarboxylate (PC) 0.3 wt.%.

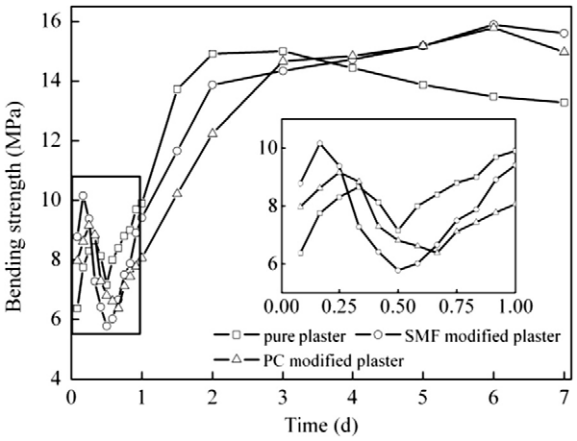

Fig. 6. Bending strength development of α-calcium sulfate hemihydrate (α-HH) based plasters, water–hemihydrate weight ratio (W/H): pure plaster 0.32, modified plasters 0.27; dosage: sulfonated melamine formaldehyde (SMF) 0.5 wt.%, polycarboxylate (PC) 0.3 wt.%.

0.25 h) in the sample with 0.5 wt.% SMF (regardless of W/H) while it occurs about 0.5 h later in the sample with 0.3 wt.% PC at W/H = 0.27, and even later at W/H = 0.32. Judging from the form of the curves, SMF accelerates the onset of plaster hydration while PC retards it. From the calorimetry curves it appears that the modified plasters with lower W/H hydrate more rapidly than those with higher W/H, but no strong conclusions can be drawn from this observation as some of the effects may simply be due to changes in the time constant of the calorimeter, which depends on the W/H used and the mass of plaster in each experiment.

Both calorimetry and set-time measurements (Table 3) suggest that SMF accelerates the hydration but PC decelerates it. It is known that the hydration of HH leading to formation of DH occurs through a solution mechanism, which involves dissolution of HH, nucleation and growth of DH crystal [14]. A part of α-HH immediately dissolves when α-HH is mixed with water, making the solution initially saturated with respect to HH and thus supersaturated with respect to DH, leading to nucleation and growth of DH crystals [7,15]. The mechanism by which an organic polymer such as PC can retard DH growth is fairly well-understood: if the polymer adsorbs strongly enough on the growing surfaces of the DH crystallites, it will block some of the growth sites and thus slow their growth. This is consistent with the reduction in growth rate observed in Figs. 4 and 5. There is no evidence for any significant delay in the nucleation, since the growth appears to start at about the same time after mixing as it does in the case of the pure plaster. It is less easy to understand how SMF can apparently accelerate DH growth. One can suggest that SMF is far less strongly adsorbed on DH growth surfaces than PC, and thus that it doesn't have any effect on the DH growth rate; but that can't explain an apparent acceleration. However, looking carefully at Fig. 5, we observe that the mixes with SMF apparently start to hydrate immediately after mixing, whereas the pure plaster and the PC-modified plaster seem to require a significant delay, which might be ascribed to the time required for nucleation of DH. It thus seems that SMF is able to accelerate the nucleation of DH; but exactly how it does so is not yet clear.

Table 3
Effect of sulfonated melamine formaldehyde (SMF) and polycarboxylate (PC) on the setting time of plasters.

Plaster	Initial setting time (min)	Final setting time (min)
Pure	7–8	13–14
SMF-modified	6–7	12–13
PC-modified	13–14	19–20

3.4. Strength development of plaster

The strength of set plaster develops during the hydration and hardening process. However, little information is available for the strength development of α-HH based set plaster. Lewry and Williamson argued that strength development of HH is a three-stage process [6]. The strength development of set plasters with and without modification is shown in detail in Figs. 6 and 7. It is found that the hydration and hardening process of plaster could be divided roughly into five stages:

I. Bond of particles in paste. When plaster is blended with water, α-HH crystals interact with each other by van der Waals molecular force through water membrane. Accordingly, a structure with rather low strength and paste with thixotropic character is formed. This stage cannot surpass the final setting of plaster (Table 3).
II. Formation of crystal matrix. In this stage, many DH nuclei emerge, grow and finally contact each other. A DH crystal matrix forms and the paste loses thixotropic character. Transformation from α-HH to DH has been completed at the end of this stage, proved by the variation of crystal water content of hydration product (Fig. 4). The matrix formation

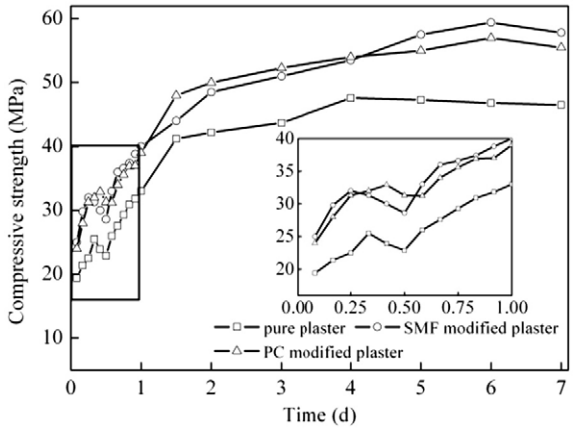

Fig. 7. Compressive strength development of α-calcium sulfate hemihydrate (α-HH) based plasters, water–hemihydrate weight ratio (W/H): pure plaster 0.32, modified plasters 0.27; dosage: sulfonated melamine formaldehyde (SMF) 0.5 wt.%, polycarboxylate (PC) 0.3 wt.%.

causes an initial rapid build-up of strength and the first strength peak occurs around 4–8 h.

III. Release of internal stress. A strength drop of 17%–43% to a minimum is observed, mainly due to excess internal stress [6]. The initial matrix formed in stage II compacts to a certain extent, and more DH crystals from different growth centers begin to push against each other. Thus, excess internal stress is generated in the matrix. When the stress exceeds the structure strength, the matrix collapses to release it.

IV. Evaporation of free water. The strength is further improved in the following days, leading to a maximum value. Along with the free water removal from the DH crystals surface by evaporation, the structure of set plaster becomes more compact, resulting in further strength increase [6]. Water loss from crystal surfaces thins out the water films between the crystals, leading to stronger adhesive forces among the DH crystals and thus the higher strength of the "dry" set plaster [16].

V. Instability of matrix joints. The strength falls slowly but irreversibly with time after it reaches the maximum value, which can be ascribed to the instability of matrix joints in moist air. In the presence of water, the matrix joints can dissolve and the DH crystals reform, and a relative creep of the crystals is enhanced [17], leading to the irreversible strength drop, which is very sensitive to atmospheric humidity.

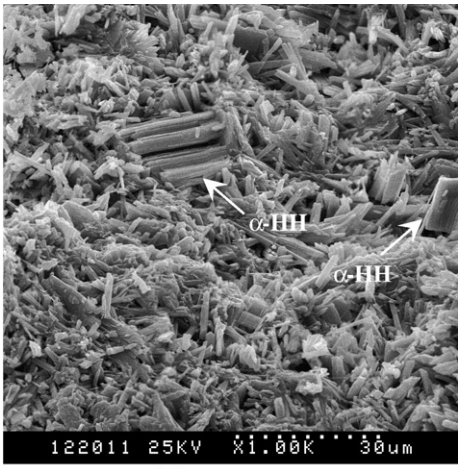

(a) Pure plaster

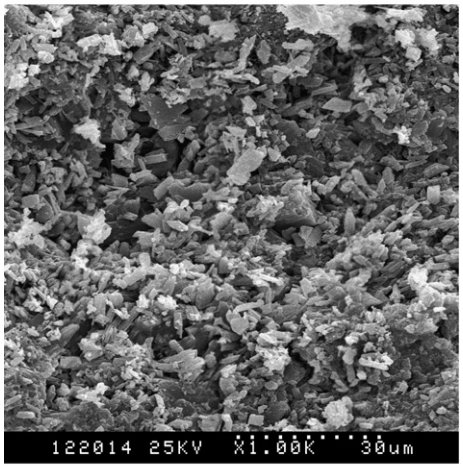

(b) SMF-modified plaster

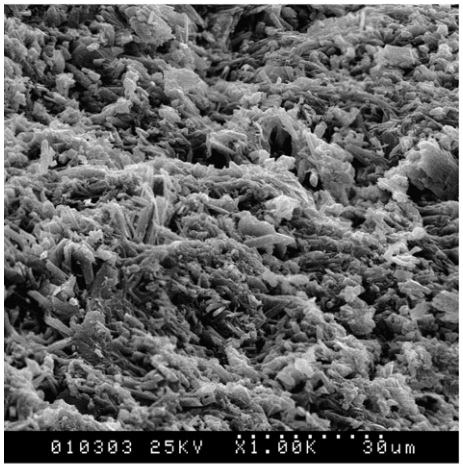

(c) PC-modified plaster

Fig. 8. Scanning Electron Microscope (SEM) image of α-calcium sulfate hemihydrate (α-HH) based plasters, water–hemihydrate weight ratio (W/H): pure plaster 0.32, modified plasters 0.27; dosage: sulfonated melamine formaldehyde (SMF) 0.5 wt.%, polycarboxylate (PC) 0.3 wt.%.

Table 4
Pore characteristics of α-calcium sulfate hemihydrate (α-HH) based set plasters.

	S_{BET} ($m^2\ g^{-1}$)	Average pore diameter (nm)	Pore volume ($cm^3\ g^{-1}$)
Pure	21.2854	10.4881	0.056990
SMF-modified	23.4175	8.1751	0.047844
PC-modified	19.6669	9.2185	0.048283

The bending strength development of modified plasters is different from that of the pure plaster (Fig. 6). The higher strength achieved by SPs is partly due to the reduction in W/H and partly due to chemical effects at the interfaces. The increase in 2 h bending strength is 38% with 0.5 wt.% SMF and 25% with 0.3 wt.% PC, and the increase in 7 day bending strength is 17% with 0.5 wt.% SMF and 13% with 0.3 wt.% PC. SMF and PC achieve, respectively, 17% and 5.8% increases in the first peak value of the strength and 5.9% and 5.2% increases in the second peak value. However, the minimum strength value and the 1 day bending strength are both lower than that of the pure plaster despite the lower W/H ratio, which is undesirable. The time of occurrence of the bending strength peak and valley also shift. SMF brings forward the first peak from 8 h to nearly 4 h, whereas PC brings forward it to about 6 h. SMF and PC both postpone the occurrence of maximum value from 2–3 days to 6 days. PC defers the valley point from 12 h to 16 h, while SMF does not. The strength fluctuation of

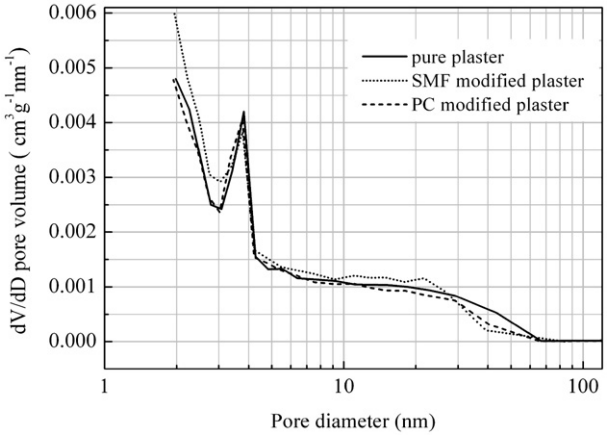

Fig. 9. Pore size and distribution of α-calcium sulfate hemihydrate (α-HH) based plasters, water–hemihydrate weight ratio (W/H): pure plaster 0.32, modified plasters 0.27; dosage: sulfonated melamine formaldehyde (SMF) 0.5 wt.%, polycarboxylate (PC) 0.3 wt.%.

modified plaster in the first day is increased and stage IV of the strength development is prolonged.

As SMF and PC both permitted a reduction in the W/H from 0.32 to 0.27, a more compact structure could form in stage II, which is responsible for the higher first peak value. Nevertheless, the more compact structure plays a negative role in bending strength development during stage III. There is less inner space for crystal growth, the internal stress increases dramatically and causes more serious structure destruction, so the minimum strength value of the modified plaster is lower than that of the pure plaster. As a result, the strength fluctuation of modified plaster in the first day is increased. The more compact structure influences stage IV as well. The evaporation of free water slows down and stage IV in modified plaster is prolonged.

The two modified plasters perform slightly different during the first day of the strength development. The occurrence time of the initial maximum and minimum strength values of the SMF-modified plaster is earlier than that of PC-modified one, which accords with the observed effects of SMF and PC on the degree of hydration. After one day or more, the strength development profiles of the modified plasters are similar to each other.

The effects of SMF and PC on compressive strength are shown in Fig. 7. The more compact structure of the matrix due to the lower water demand of plaster leads to a significantly higher final compressive strength. The general effects are similar to the effects observed in bending strength, but the compressive strength is less sensitive to the early-age changes.

3.5. Microstructure of set plaster

Properties of set plaster depend greatly on the characteristics of microstructure, such as crystal morphology and size, properties of matrix joints and pore structure [18]. Set plaster after 2 h hydration is a porous product which mainly consists of randomly orientated column-shape crystals (Fig. 8). The DH crystals in the pure plaster show a long column shape with average length of 6–8 μm and diameter of 0.3–0.5 μm (Fig. 8a). Some unhydrated α-HH crystals can also be detected with length of 20–30 μm and diameter of 10–15 μm. The crystal matrix looks loose with disordered crystals. The DH crystals in SMF-modified set plaster are still mostly column-shape, but some platy crystals are also visible (Fig. 8b), along with some apparently gelatinous substances material. Compared with those in the pure plaster, the DH crystals in the SMF-modified plaster appear about half as long and overlap closely. No α-HH crystals could be clearly detected in this compact structure. In the PC-modified plaster, the DH crystals are mainly present as plates and short columns with much gelatinous material in the matrix (Fig. 8c). The structure looks more compact than that of the pure plaster, but not as tidy as that of the SMF-modified plaster. Obviously, the DH crystals in modified set plasters are shortened and much closer to each other than those in the pure set plaster.

DH belongs to monoclinic crystal system. Ca^{2+} linking with $[SO_4]^{2-}$ tetrahedrons forms a double-layer structure, and water molecules distribute between the layers. The binding mode and energy of Ca^{2+} and $[SO_4]^{2-}$ on each axis are different, so the crystal growth rate varies with axis, resulting in formation of different faces. Promoted by bond of Ca^{2+} and $[SO_4]^{2-}$ on two free ends, the faces on *c*-axis grow most rapidly, resulting in the formation of column-shape crystals [19]. These faces, which mainly consist of Ca^{2+}, attract functional ion groups of SP preferentially when SP is added, leading to the formation of gelatinous substance. Thus, surface energy of these faces falls and growth of these faces slows down, which finally changes the crystal shape.

In previous studies on cementitious materials, pore distribution and porosity were usually determined by mercury intrusion [20,21]. However, in these α-HH based plasters the pores were apparently too small to be intruded by mercury, so we instead used the BET method to study the pore characteristics (Table 4 and Fig. 9). The characteristic pore size of the set plaster was 3–4 nm, which varies little with the addition of SPs. Compared with the pure plaster, pores smaller than 3 nm and in the range of 4–26 nm increase while pores larger than 26 nm decrease in SMF-modified plaster. That is, the pores are homogenized by SMF. Comparatively, in PC-modified plaster, pores smaller than 10 nm vary little while pores larger than 10 nm decrease. A more compact structure is obtained by SMF or PC, the average pore diameter of set plaster is decreased 22% by SMF and 12% by PC, the total pore volume is decreased 16% by SMF and 15% by PC, while the BET surface area varies a little. The pore properties of set plaster are obviously in accordance with the microstructure of set plaster by SEM analysis (Fig. 8).

4. Conclusions

Two different types of superplasticizers, SMF and PC, can both be used as water-reducing agents to decrease the water demand of plaster for standard consistency. The water-reducing efficiency for the plaster reaches a maximum of 15.6% at 0.5 wt.% SMF or 0.3 wt.% PC, these SP dosages being considered optimal. The resulting increase in the 2 h bending strength is 38% with SMF and 25% with PC in comparison with the pure plaster.

The XPS spectra of $Ca2p_{3/2}$ indicate SMF and PC are both chemically adsorbed on gypsum surface in the form of monolayers owing to the electronegativity of the functional ion groups of SPs. The optimum dosage of SMF depends on its saturated adsorption amount on gypsum surface, but the variation of Ca2p/S2p ratio cannot indicate the optimum dosage of PC because of Ca^{2+} bonding with both of $[R\text{-}COO]^-$ and $[R\text{-}SO_3]^-$.

The hydration and hardening process of plaster could be divided roughly into five stages: I. Bond of particles in paste; II. Formation of crystal matrix; III. Release of internal stress; IV. Evaporation of free water; V. Instability of matrix joints. The strength development profiles of the two modified plasters are extremely similar, but differ from that of the pure plaster. SMF accelerates the hydration, while PC decelerates it, leading to higher strength of SMF-modified plaster in the initial period.

SPs can reduce the water demand of α-HH, shorten the DH crystals, increase the crystal overlapping, and decrease the total pore volume and average pore diameter of the set plaster. Therefore, more compact structures and higher strengths can be obtained by means of SPs, and SMF works better than PC.

Acknowledgements

The authors are grateful for the financial support by the Hi-Tech Research and Development Program of China (No. 2006AA03Z385), the Science and Technology Plan of Zhejiang Province, China (No. 2007C23055) and the New Century Excellent Scholar Program of Ministry of Education of China (NCET-04-0549).

References

[1] A.M. Grabiec, Contribution to the knowledge of melamine superplasticizer effect on some characteristics of concrete after long periods of hardening, Cem. Concr. Res. 29 (5) (1999) 699–704.
[2] N. Mikanovic, C. Jolicoeur, Influence of superplasticizers on the rheology and stability of limestone and cement pastes, Cem. Concr. Res. 38 (7) (2008) 907–919.
[3] S. Eve, M. Gomina, J. Hamel, G. Orange, Investigation of the setting of polyamide fibre/latex-filled plaster composites, J. Eur. Ceram. Soc. 26 (13) (2006) 2541–2546.
[4] J.C. Rubio-Avalos, A. Manzano-Ramírez, J.G. Luna-Bárcenas, J.F. Pérez-Robles, E.M. Alonso-Guzmán, M.E. Contreras-García, J. González-Hernández, Flexural behavior and microstructure analysis of a gypsum-SBR composite material, Mater. Lett. 59 (2–3) (2005) 230–233.
[5] P. Jiahui, Q. Jindong, Z. Jianxin, C. Mingfeng, W. Tizhi, Adsorption characteristics of water-reducing agents on gypsum surface and its effect on the rheology of gypsum plaster, Cem. Concr. Res. 35 (3) (2005) 527–531.
[6] A.J. Lewry, J. Williamson, The setting of gypsum plaster. Part II: The development of microstructure and strength, J. Mater. Sci. 29 (21) (1994) 5524–5528.

[7] N.B. Singh, B. Middendorf, Calcium sulphate hemihydrate hydration leading to gypsum crystallization, Prog. Cryst. Growth Charact. Mater. 53 (1) (2007) 57–77.
[8] C. Legrand, E. Wirquin, Influence of superplasticizer dosage on the quantity of hydrates needed to obtain a given strength for very young concrete, Mater. Struct. 27 (1994) 135–137.
[9] T. Sebok, M. Vondruska, Interaction of anhydrite and melamine-formaldehyde polycondensates in aqueous suspensions, Cem. Concr. Res. 30 (6) (2000) 993–1003.
[10] K. Yamada, S. Ogawa, S. Hanehara, Controlling of the adsorption and dispersing force of polycarboxylate-type superplasticizer by sulfate ion concentration in aqueous phase, Cem. Concr. Res. 31 (3) (2001) 375–383.
[11] B. Demri, D. Muster, XPS study of some calcium compounds, J. Mater. Process. Technol. 55 (3–4) (1995) 311–314.
[12] M. Collepardi, V.S. Ramachandran, Effect of Admixtures, 9th International Congress on the Chemistry of Cement, New Delhi, India, 1992 p. 529–570.
[13] K. Yamada, T. Takahashi, S. Hanehara, M. Matsuhisa, Effect of the chemical structure on the properties of polycarboxylate-type superplasticizer, Cem. Concr. Res. 30 (2) (2000) 197–207.
[14] A.J. Lewry, J. Williamson, The setting of gypsum plaster. Part I: The hydration of calcium sulphate hemihydrate, J. Mater. Sci. 29 (20) (1994) 5279–5284.
[15] E.M. Gartner, J.M. Gaidis, Hydration Mechanisms I, in: J. Skalny (Ed.), Mater. Sci. Concr., vol. I, American Ceramic Society, Westerville, 1989, p. 95.
[16] J. Chappuis, A new model for a better understanding of the cohesion of hardened hydraulic materials, Colloids Surf., A 156 (1–3) (1999) 223–241.
[17] P. Reynaud, M. Saâdaoui, S. Meille, G. Fantozzi, Water effect on internal friction of set plaster, Mater. Sci. Eng., A 442 (1–2) (2006) 500–503.
[18] M. Singh, M. Garg, Relationship between mechanical properties and porosity of water-resistant gypsum binder, Cem. Concr. Res. 26 (3) (1996) 449–456.
[19] S. Follner, A. Wolter, K. Helming, C. Silber, H. Bartels, H. Follner, On the real structure of gypsum crystals, Cryst. Res. Technol. 37 (2–3) (2002) 207–218.
[20] S. Eve, M. Gomina, J.-P. Jernot, J.-C. Ozouf, G. Orange, Microstructure characterization of polyamide fibre/latex-filled plaster composites, J. Eur. Ceram. Soc. 27 (12) (2007) 3517–3525.
[21] D.A. Silva, V.M. John, J.L.D. Ribeiro, H.R. Roman, Pore size distribution of hydrated cement pastes modified with polymers, Cem. Concr. Res. 31 (8) (2001) 1177–1184.